**Title:** **Human cerebrospinal fluid promotes spontaneous gamma oscillations in the hippocampus *in vitro***

**Running title:** Human CSF promotes hippocampal gamma oscillations

**Authors:** Andreas Bjorefeldt[1,2†], Firoz Roshan[3†], My Forsberg[1], Henrik Zetterberg[4,5,6,7], Eric Hanse[1‡] & André Fisahn[3‡]

**Affiliations:**

*1 Department of Physiology, Institute of Neuroscience and Physiology, University of Gothenburg, Box 432, 405 30, Gothenburg, Sweden.*

*2 Department of Neuroscience, Brown University, Providence, RI 02912, United States.*

*3 Neuronal Oscillations Laboratory, Center for Alzheimer Research, Department of Neurobiology, Care Sciences and Society, Karolinska Institutet, 17177 Stockholm, Sweden.*

*4 Department of Psychiatry and Neurochemistry, Institute of Neuroscience and Physiology, University of Gothenburg, 431 80 Molndal, Sweden.*

*5 Clinical Neurochemistry Laboratory, Sahlgrenska University Hospital, 431 80 Molndal, Sweden.*

*6 Department of Neurodegenerative Disease, UCL Institute of Neurology, Queen Square, WC1N 3BG London, UK.*

*7 UK Dementia Research Institute at UCL, London WC1E 6BT, UK.*

*† ‡ authors contributed equally to this work*

**Key words:** hippocampal brain slice, neuromodulation, CSF, pyramidal cell, fast-spiking interneuron

**Corresp. author:** Dr. Andreas Bjorefeldt
Medicinaregatan 11
Box 432
405 30 Gothenburg
Sweden
Email: andreas.bjorefeldt@gu.se.

**Number of pages:** 43
**Number of figures:** 5
**Number of tables:** 1

## FUNDING INFORMATION

A.B. was supported by Swedish Research Council 2016-06760, H.Z. by Swedish Research Council 2013-2546, Swedish State Support for Clinical Research ALFGBG-441051, European Research Council 681712 and the Knut and Alice Wallenberg Foundation (WAF2013), E.H. by Swedish Research Council 2016-00986, Swedish State Support for Clinical Research ALFGBG-427611, Alzheimerfonden AF-640391 and the Swedish Brain Foundation F02017-0035 and A.F. by Swedish Research Council 2014-3191, Swedish brain foundation FO2015-0132, Åhlén Foundation mC2/h14, Alzheimerfonden AF-556351 and the Strategic Program in Neurosciences at the Karolinska Institute.

## ABSTRACT

Gamma oscillations (30–80 Hz) are fast network activity patterns frequently linked to cognition. They are commonly studied in hippocampal brain slices *in vitro*, where they can be evoked via pharmacological activation of various receptor families. One limitation of this approach is that neuronal activity is studied in a highly artificial extracellular fluid environment, as provided by artificial cerebrospinal fluid (aCSF). Here we examine the influence of human cerebrospinal fluid (hCSF) on kainate-evoked and spontaneous gamma oscillations in mouse hippocampus. We show that hCSF, as compared to aCSF of matched electrolyte and glucose composition, increases the power of kainate-evoked gamma oscillations and induces spontaneous gamma activity that is reversed by washout. Bath application of atropine entirely abolished hCSF-induced gamma oscillations, indicating critical contribution from

muscarinic acetylcholine receptor-mediated signaling. In separate whole-cell patch clamp recordings from rat hippocampus, hCSF increased theta resonance frequency and strength in pyramidal cells along with enhancement of h-current ($I_h$) amplitude. Fast-spiking interneurons did not show intrinsic gamma frequency resonance at baseline (aCSF), and this was not altered by hCSF. However, hCSF increased the excitability of these interneurons, which, together with an enhancement of $I_h$ in pyramidal cells, is likely to contribute to hCSF-induced spontaneous gamma oscillations. Our findings show that hCSF promotes gamma rhythmicity in the hippocampus and suggest that neuromodulators distributed in CSF could significantly influence neuronal network activity *in vivo*.

## INTRODUCTION

Mammalian brains produce multiple types of synchronized network oscillations at frequencies spanning 0–400 Hz (Buzsaki, 2006; Buzsaki and Draguhn, 2004). Network oscillations in the gamma frequency-band (30–80 Hz), also known as gamma oscillations, have received significant attention over the last two decades as they (1) positively correlate with, and can predict, cognitive performance in humans and animals (Beshel et al., 2007; Sederberg et al., 2007; Taylor et al., 2005; Yamamoto et al., 2014), and (2) provide a putative mechanism for information coding and transfer in the brain (Fries, 2015; Lisman and Jensen, 2013; Singer, 1999). Whether gamma oscillations are critically involved in information processing, or merely constitute inevitable by-products of activated neuronal networks, is of much current interest (Cardin, 2016; Sohal, 2016).

It is well established that gamma oscillations arise from temporally precise coordination of excitatory and inhibitory synaptic potentials in neuronal networks consisting of principal cells and GABAergic interneurons, leading to rhythmic membrane potential fluctuations in the population. At the cellular level, fast-spiking (FS) parvalbumin-positive interneurons are thought to have a specialized role in orchestrating these oscillations (Buzsaki and Wang, 2012; Sohal et al., 2009). Optogenetic activation or silencing of these neurons *in vivo* promotes and inhibits cortical gamma oscillations, respectively (Cardin et al., 2009; Sohal et al., 2009). A number of structural and functional properties of FS interneurons are thought to underlie their ability to facilitate gamma rhythms. Notably, these cells are heavily interconnected both through electrical gap junctions and reciprocal inhibitory synapses, and further innervate themselves via inhibitory autapses (Bacci et al., 2003; Tamas et al., 1997). Moreover, they form powerful perisomatic-targeting GABAergic synapses onto principal cells, enabling high temporal precision control of their firing. Some of the unique functional properties of FS interneurons include short membrane time constants, low input resistance, high (≥ 150 Hz) maximal firing frequencies and intrinsic gamma frequency resonance (Pike et al., 2000). Although an interconnected network of FS interneurons can be sufficient to produce gamma oscillations (Traub et al., 1996; Whittington et al., 1995), phasic excitation provided by principal cells is likely essential to their generation *in vivo* (Fisahn et al., 1998; Fuchs et al., 2007; Mann et al., 2005). By regulating the strength and synchronicity of their action potential output, principal cells may control the recruitment of local FS interneurons and thereby the strength of the network oscillation.

Gamma oscillations are frequently studied in rodent hippocampal brain slices *in vitro*, where they can be chemically evoked via pharmacological activation of various receptor families such as kainate receptors (Flint and Connors, 1996), muscarinic receptors (Fisahn et al., 1998) or metabotropic glutamate receptors (Boddeke et al., 1997; Palhalmi et al., 2004). The hippocampal circuitry mechanisms responsible for the generation of gamma oscillations are conserved across the commonly used rodent species – mouse and rat (Fisahn et al., 2004; Fisahn et al., 1998; Fisahn et al., 2002).

While experiments in brain slices have helped reveal invaluable insights into cellular and synaptic mechanisms of these oscillations, a limitation of these studies is that neuronal activity is routinely recorded in an artificial extracellular environment, as provided by artificial cerebrospinal fluid (aCSF). We recently found that human cerebrospinal fluid (hCSF) contains organic neuromodulators that markedly increase the excitability of both hippocampal CA1 pyramidal cells (Bjorefeldt et al., 2015) and interneurons (Bjorefeldt et al., 2016), raising the possibility that hCSF may promote synchronized network activity in the hippocampus. Here we address this question by examining the influence of hCSF, as compared to electrolyte and glucose-matched aCSF, on gamma oscillatory network activity in the *in vitro* rat hippocampal brain slice preparation.

## MATERIALS AND METHODS

### Local field potential recordings

149 *Animals*

150 Experiments were carried out in accordance with the ethical permit granted by Norra
151 Stockholms Djurförsöksetiska Nämnd to AF (N45/13). C57BL/6 mice of either sex
152 (postnatal day 14–23, supplied from Charles River, Germany) were used in all
153 experiments. The animals were deeply anaesthetized with isoflurane before being
154 sacrificed by decapitation.

155

156 *Tissue preparation*

157 The brain was dissected out and placed in ice-cold aCSF modified for dissection.
158 This solution contained (in mM): 80 NaCl, 24 $NaHCO_3$, 25 Glucose, 1.25 $NaH_2PO_4$, 1
159 Ascorbic acid, 3 NaPyruvate, 2.5 KCl, 4 $MgCl_2$, 0.5 $CaCl_2$ and 75 Sucrose.
160 Horizontal sections (350 µm thick) from both hemispheres were prepared with a
161 Leica VT1200S vibratome (Microsystems, Stockholm, Sweden). Immediately after
162 slicing, sections were transferred to a submerged incubation chamber containing
163 standard aCSF (in mM): 124 NaCl, 30 $NaHCO_3$, 10 Glucose, 1.25 $NaH_2PO_4$, 3.5
164 KCl, 1.5 $MgCl_2$ and 1.5 $CaCl_2$. The chamber was held at 34 °C for at least 20
165 minutes after dissection. It was subsequently allowed to cool to ambient room
166 temperature for a minimum of 40 minutes. While in the chamber, the slices were
167 continuously supplied with carbogen gas (5% $CO_2$, 95% $O_2$).

168

169 *Electrophysiology*

170 Recordings were carried out in hippocampal area CA3 with borosilicate glass
171 microelectrodes pulled to a resistance of 3–5MΩ. Local field potentials (LFP) were
172 recorded in an interface-type chamber (perfusion rate 4.5 ml/min) at 34 °C using
173 microelectrodes filled with aCSF placed in stratum pyramidale. The slices were

allowed to stabilize in hCSF for 30 minutes before any recordings were made. LFP gamma oscillations were either observed to occur spontaneously in hCSF or elicited by applying 25 nM kainate (KA) to the extracellular bath. In the latter case they were allowed to stabilize for 25 minutes prior to recordings. KA concentration was increased in 10 nM steps to reach a concentration of 45 nM, with a 25 min stabilization period following each application. The interface chamber recording solution contained aCSF or hCSF of varying composition (see section 'Human and artificial cerebrospinal fluid' below).

Interface chamber LFP recordings were performed with a 4-channel amplifier / signal conditioner M102 amplifier (Electronics lab, Faculty of Mathematics and Natural Sciences, University of Cologne, Cologne, Germany). The signals were sampled at 10 kHz, conditioned using a Hum Bug 50 Hz noise eliminator (LFP signals only; Quest Scientific, North Vancouver, BC, Canada), software low-pass filtered at 1 kHz, digitized and stored using a Digidata 1322A and Clampex 9.6 software (Molecular Devices, CA, USA).

*Data analysis*

Power spectral density plots obtained from 60-s long LFP recordings were calculated in averaged Fourier-segments of 8192 points, which reduces 1/f noise (Axograph X, Kagi, Berkeley, CA, USA). Oscillatory power was calculated by integrating the power spectral density between 20 and 80 Hz. The low cut-off frequency of 20 Hz was chosen because the recording temperature (34 °C) is lower than mouse body temperature and gamma oscillation frequency decreases by approximately 3.5 Hz

for each 1 °C temperature decrease (Andersson et al., 2010; Dickinson et al., 2003; Kurudenkandy et al., 2014).

*Drugs and chemicals*

Drugs were bath-applied at indicated concentrations. KA was obtained from Tocris. Atropine as well as chemicals and salts used in extracellular solutions and micropipettes were obtained from Sigma-Aldrich.

## Whole-cell patch clamp recordings

*Animals*

Experiments were performed in hippocampal brain slices prepared from 15–30 day-old (P15–30) Wistar rats with permission from the local ethical committee for animal research at the University of Gothenburg, Sweden (29/2014). Male and female rats were deeply anaesthetized via inhalation of isoflurane (Abbott) and then decapitated.

*Tissue preparation*

Brains were quickly isolated and submerged in ice-cold (0–3 °C) slicing solution containing (in mM): 220 Glycerol, 2.5 KCl, 1.2 $CaCl_2$, 7 $MgCl_2$, 26 $NaHCO_3$, 1.2 $NaH_2PO_4$ and 11 Glucose. Horizontal hippocampal slices (300–400 $\mu$m) were prepared from both hemispheres using a vibratome (Microm, HM650V). Brain slices were then stored in a holding chamber containing (in mM): 129 NaCl, 3 KCl, 2 $CaCl_2$, 4 $MgCl_2$, 26 $NaHCO_3$, 1.25 $NaH_2PO_4$ and 10 Glucose. Both slicing and storage solutions were continuously bubbled with carbogen gas (95% $O_2$, 5% $CO_2$). Slices

were stored for a period of 1–5 hours at room temperature (22–25 °C) before transferred to a recording chamber perfused with aCSF at a rate of 3 ml/min.

*Electrophysiology*

Whole-cell recordings were made from CA1 pyramidal cells and FS interneurons under visual guidance using differential interference contrast microscopy (Nikon E600FN) together with a CCD camera (Sony XC-73CE). Borosilicate glass micropipettes with resistances of 3–5 MΩ were prepared using a P-97 horizontal micropipette puller (Sutter instruments). The intracellular solution used in whole-cell voltage and current clamp recordings contained (in mM): 127 $K^+$-gluconate, 8 KCl, 10 HEPES, 15 Phosphocreatine, 4 Mg-ATP, 0.3 Na-GTP (pH 7.35, 300 mOsm/Kg). Pipette capacitance was cancelled in cell-attached mode. After entering whole-cell configuration, no current or voltage was applied to the cell during the first two minutes. Series resistances ranged from 5–20 MΩ and were not compensated. Recordings in which the series resistance changed more than 20% were discarded. Membrane potentials were corrected for a measured liquid junction potential of –9 mV. Data was acquired at a sampling frequency of 10 kHz and filtered at 3 kHz using an EPC-9 amplifier combined with the PatchMaster software (HEKA Elektronik). All experiments were performed at a recording temperature of 32–34 °C.

Theta resonance in CA1 pyramidal cells was examined at –85 mV by injecting a sinusoidal current of constant amplitude and linearly increasing frequency (ZAP current) in current-clamp mode for 30 s (0–15 Hz, 40 pA). CA1 pyramidal cells were also tested for a gamma resonance peak at 35–40 Hz using a second ZAP current protocol (20–60 Hz, 40 pA, 30 s). The hyperpolarization-activated cation current, $I_h$,

was recorded using a two-step voltage-clamp protocol where hyperpolarizing voltage commands (–80 to 0 mV, 10 mV decrements, 3 s) were given from a holding potential of –40 mV (Maccaferri and McBain, 1996). After each voltage step $I_h$ was then fully activated by a second step to –120 mV, producing slowly relaxing tail currents. The amplitude of $I_h$ in response to the first voltage step was normalized to the tail current amplitude at full activation. In FS CA1 interneurons, sinusoidal current waveforms of constant frequency were delivered at 5, 40 and 100 Hz (20 pA, 5 s) from –60 mV, in 10 pA increments. ZAP currents (0–100 Hz, 20 pA, 20 s) were also injected at near-threshold membrane potential (–45 to –50 mV).

*Data analysis*

All data analysis was performed in IGOR Pro (version 6, WaveMetrics). Electrical resonance was characterized using the impedance (Z) amplitude profile (ZAP) method (Hu et al., 2002; Puil et al., 1986). Impedance magnitude was plotted as a function of frequency by dividing the fast Fourier transform (FFT) of the voltage response with the FFT of the driving current:

$$Z = FFT(V)/FFT(I)$$

The electrical resonance frequency was measured at the peak impedance of the voltage response to ZAP current injection. Resonance strength (Q-value) was quantified as the ratio between the impedance at resonance frequency and the impedance at 0.5 Hz. Absence of electrical resonance manifests as a Q-value of 1, where the peak impedance of the voltage response occurs at the lowest input frequency (0.5 Hz).

$I_h$-amplitude was quantified as the difference between the instantaneous current and the current measured at steady-state. Experiments were performed in absence of intrinsic channel blockers to allow possible effects of hCSF on this conductance to be correlated to effects on resonance. The maximal evoked firing frequency, input resistance and sag ratio of FS interneurons was calculated from voltage responses to hyperpolarizing and depolarizing square current pulses (800 ms, 50 pA increments) delivered from –70 mV. Sag ratio was calculated by dividing the steady state amplitude during a hyperpolarizing current injection (–100 pA) with the maximum amplitude. In FS interneuron recordings where sinusoidal current waveforms of constant frequency were injected, the sweep closest to threshold was used for impedance magnitude analysis.

*Drugs and chemicals*

D-(-)-2-Amino-5-phosphonopentanoic acid (D-AP5) and 6-cyano-7-nitroquinoxaline-2,3-dione (CNQX) and picrotoxin (PTX) were added to all recording aCSF and hCSF solutions to block fast glutamatergic, and GABAergic, synaptic transmission. In recordings from CA1 pyramidal cells, the aCSF and hCSF were further supplemented with tetrodotoxin (TTX) to block voltage-gated sodium channels. Drugs were purchased from Sigma-Aldrich and bath-applied at the following concentrations: 50 µM D-AP5, 15 µM CNQX, 50 µM PTX and 0.5 µM TTX. Additional chemicals and salts used in intra- and extracellular solutions were purchased from Sigma-Aldrich.

**Human and artificial cerebrospinal fluid**

hCSF samples were acquired from patients diagnosed with normal pressure hydrocephalus (NPH) and healthy control subjects through a lumbar puncture procedure performed by neurologists at the Sahlgrenska University Hospital in Gothenburg, Sweden. Healthy hCSF was obtained from male and female volunteers after written informed consent, and with permission from the local ethical committee at the University of Gothenburg (no. 942-12). Separate pools of patient and healthy control hCSF were created from 5-10 individual samples, the volume of each ranging from 15-50 ml. hCSF from 4 pools, each between 150-500 ml, were used (3 NPH pools, 1 healthy control pool). As both patient and healthy hCSF had similar effects on gamma power, data from these two sources was combined. No direct comparison of effect strength of patient and healthy hCSF was made as this was not the focus of the present study. Newly acquired hCSF samples were centrifuged (2000 r.p.m., 10 min) and quickly transferred to a –80 $^{o}$C freezer and stored until a sufficient volume had been collected. Collected samples were then thawed, pooled and aliquoted into 50 ml falcon tubes that were shipped on dry ice to Karolinska Institutet in Stockholm. Part of the pooled hCSF was refrozen at a –80 $^{o}$C and kept at the Sahlgrenska Academy in Gothenburg to be used in whole-cell patch clamp recordings. Electrolyte and glucose concentrations, as well as pH and osmolality, were measured according to methodology described in Bjorefeldt et al. (2015). A matched aCSF was then prepared based on measured hCSF values, and used as control. All hCSF pools used showed normal electrolyte and glucose content, pH, osmolality and coloring. The ionized fractions of $Ca^{2+}$ and $Mg^{2+}$ in hCSF were estimated to account for 90% of the measured total concentrations (Joborn et al., 1991). On experimental day hCSF was thawed to room temperature in a bowl of warm (37 $^{o}$C) water. Both aCSF

and hCSF were bubbled with carbogen gas (95% $O_2$, 5% $CO_2$) in electrophysiological recordings, and for a minimum of 5 min prior to pH measurements on pooled hCSF. The volume of hCSF used in a single experiment ranged from 12–25 ml in this study.

**Statistics**

A paired samples design was used throughout the study. In local field potential recordings, 3–4 brain slices were recorded in parallel in different channels (6–8 slices per animal, n = number of slices). In patch clamp experiments, recordings were attempted from 1–5 neurons per brain slice (6–8 slices per animal, n = number of cells). The paired Student's t-test was used for evaluating statistical significance in all experiments using SPSS (Version 22, IBM). Significance levels are given as *** $p < 0.001$; ** $p < 0.01$; * $p < 0.05$. Data is reported as mean ± standard error of the mean.

**RESULTS**

**hCSF increases the power of kainate-induced gamma oscillations**

We first examined the effect of hCSF on KA-induced gamma oscillations in CA3 stratum pyramidale, a well-established method for studying these oscillations *in vitro* (Fisahn, 2005). Previous work has shown that hCSF increases the excitability of both hippocampal pyramidal cells (Bjorefeldt et al., 2015) and interneurons (Bjorefeldt *et al.*, 2016), raising the possibility that synchronized neuronal activity might be

promoted. Step application of 25, 35 and 45 nM KA to aCSF (of matched composition with regard to hCSF, see Methods) successively evoked gamma oscillations of increasing power (from 1.33 ± 0.11 x $10^{-09}$ $V^2$ to 4.13 ± 0.11 x $10^{-09}$ $V^2$ (n = 9, Figure 1). Following a 25 min stabilization period at 45 nM KA, gamma oscillations were completely stable over a 5 min recording period before hCSF was introduced. Wash-in of hCSF supplemented with 45 nM KA substantially strengthened gamma oscillations from 4.13 ± 0.11 x $10^{-09}$ $V^2$ to 7.25 ± 0.11 x $10^{-09}$ $V^2$ (n = 9, P < 0.001, Student's paired t-test, Figure 1), suggesting the possibility of a synchronization-promoting effect of hCSF.

**hCSF promotes spontaneous gamma oscillations**

Given that hCSF potently increased the power of KA-induced gamma oscillations we next tested whether hCSF alone was able to elicit oscillatory activity in stratum pyramidale of the major hippocampal subfields CA3 and CA1. Slices were first allowed to rest for 30 min in matched aCSF before any recordings were made. No spontaneous gamma oscillations were observed in aCSF and power spectral analysis showed absence of gamma frequency peaks. After switching from aCSF (of matched electrolyte/glucose composition) to hCSF, spontaneous gamma oscillations started to appear within 5 min (no KA or other drugs were added). Recordings commenced after a 20 min wash-in period of hCSF and revealed in area CA3 gamma oscillation power of 1.67 ± 0.13 x $10^{-09}$ $V^2$, compared to 0.63 ± 0.38 x $10^{-09}$ $V^2$ in aCSF (n = 11, P < 0.001, Student's paired t-test, Figure 2a-c). The increase in gamma power was entirely reversed after 25 min of washout with aCSF (0.67 ± 0.38 x $10^{-09}$ $V^2$, n = 11, P < 0.001, Student's paired t-test, Figure 2a-c).

The corresponding values for the gamma oscillation recordings in area CA1 were gamma oscillation power of 0.64 ± 0.1 x $10^{-09}$ $V^2$, compared to 0.18 ± 0.02 x $10^{-09}$ $V^2$ in aCSF (n = 6, P = 0.005, Student's paired t-test, Figure 2d-f). The increase in gamma power was entirely reversed after 25 min of washout with aCSF (0.22 ± 0.3 x $10^{-09}$ $V^2$, n = 6, P = 0.05, Student's paired t-test, Figure 2d-f). The lesser strength of spontaneous gamma oscillations recorded in area CA1 vs area CA3 is consistent with earlier results obtained with chemically-induced gamma oscillations and the location of the major gamma generator in area CA3 (Fisahn et al., 1998).

The average strength of the hCSF-induced gamma oscillations was comparable to that seen in aCSF supplemented with 25 nM KA (cf. Figure 1). There was, however, considerable variability in the strength of these oscillations between slices. In approximately 30% of examined slices, hCSF-induced gamma oscillations were especially prominent with distinct power spectrum peaks in the 35–40 Hz range. In the other examined slices, the increase in gamma power caused by hCSF was of low to moderate size. Nonetheless, we found that presence of hCSF consistently resulted in the emergence of spontaneous gamma oscillations in all recordings.

**Gamma oscillations induced by hCSF are abolished by atropine**

Previous work has shown that hippocampal network oscillations are closely associated with the neuromodulator acetylcholine (ACh) both *in vivo* (Vandecasteele et al., 2014) and *in vitro* (Fisahn et al., 1998). Given the recognized contribution of ACh to hippocampal network patterns *in vivo*, we next examined the cholinergic

dependence of the hCSF-induced gamma oscillations. In these experiments, hippocampal slices were directly transferred to a recording chamber perfused with hCSF. Following a 30 min stabilization period, spontaneous gamma oscillations of varying strength could be observed (Figure 3a). After recording stable activity over 5 min, atropine (5 µM) was applied to the hCSF perfusate. Over 5–10 min, atropine strongly reduced gamma power from 1.1 ± 0.1 x $10^{-09}$ $V^2$ to 0.39 ± 0.5 x $10^{-09}$ $V^2$ (n = 9, P = 0.0007, Student's paired t-test, Figure 3a-c).

**hCSF enhances theta resonance and increases $I_h$-amplitude in hippocampal pyramidal cells**

To examine a cellular mechanism that could help explain the appearance of gamma oscillations in hCSF, we tested the effect of hCSF on electrical resonance properties in hippocampal CA1 pyramidal cells. Cells were current-clamped at –85 mV and injected with sinusoidal current waveforms of linearly increasing frequency (ZAP currents). Two different protocols were used to characterize the effect of hCSF on the ZAP response at both theta and gamma frequencies. ZAP current injection at theta frequency range (0–15 Hz, 30 s) confirmed presence of electrical theta resonance in CA1 pyramidal cells (Figure 4a-d), as has been previously described (Hu et al., 2002; Pape, 1996). We found that hCSF caused a small yet significant increase in theta resonance frequency (from 5.1 ± 0.5 Hz to 5.9 ± 0.6 Hz, n = 8, P = 0.016, Student's paired t-test, Figure 4c), and decreased the impedance magnitude (Z) at resonance frequency (84.9 ± 7.9 MΩ vs 63.4 ± 9.8 MΩ, n = 8, P = 0.014, Student's paired t-test, Figure 4b). The effect of hCSF on Z was frequency-dependent and was not significant at 15 Hz (58.2 ± 5.2 MΩ vs 52.2 ± 4.6 MΩ, n = 8,

P = 0.08, Student's paired t-test, Figure 4b). We also found a small increase in theta resonance strength (Q-value) of CA1 pyramidal cells in hCSF (from 1.21 ± 0.02 to 1.24 ± 0.03, n = 8, P = 0.026, Student's paired t-test, Figure 4d). ZAP current injection at gamma frequency range (20–60 Hz, 30 s) showed no evidence of gamma resonance in CA1 pyramidal cells in either aCSF or hCSF (Figure 4e-f). However, a frequency-dependent effect of hCSF on Z was observed also in the 20–60 Hz range (Δ5.7 ± 0.7 MΩ at 20 Hz; Δ1.9 ± 0.7 MΩ at 60 Hz, n = 8, P = 0.004, Student's paired t-test, Figure 4f).

The frequency-dependent effect of hCSF on Z, together with the increased resonance strength observed at theta frequency, indicated that hCSF might positively modulate $I_h$. To test for a potential effect of hCSF on $I_h$, hyperpolarizing voltage steps were elicited from a holding potential of –40 mV in voltage-clamp mode (Figure 4g). Because these experiments were performed in absence of hyperpolarization-activated cyclic nucleotide–gated (HCN) channel blocker (to correlate effects of hCSF on resonance with effects on $I_h$ in matched recordings), we restricted our analysis to more hyperpolarized potentials to minimize possible contamination by other voltage-dependent conductances. Activation of $I_h$ produced a slow inward relaxation that reached steady-state amplitude over three seconds (Figure 3g). Activation curves showed that hCSF did not alter the voltage-dependence of $I_h$ between –80 and –120 mV (Figure 4h), but significantly increased the maximum current amplitude (+19.2 ± 7% at -120 mV, n = 8, P = 0.018, and +14.9 ± 4% at -100 mV, n = 8, P = 0.02, Student's paired t-tests, Figure 4i).

**hCSF enhances excitability in hippocampal fast-spiking interneurons in**

**absence of intrinsic gamma resonance**

We next tested a potential interneuronal mechanism that could help explain how hCSF promotes gamma oscillations in the hippocampal network. FS CA1 interneurons have previously been shown to display voltage-gated sodium channel-dependent gamma frequency resonance in horizontal hippocampal slices from rat (Pike et al., 2000), and we reasoned that augmentation of this intrinsic property by hCSF may contribute to generating network gamma activity. Cells with somata in CA1 stratum pyramidale, and bordering stratum oriens, were visually targeted for whole-cell patch clamp experiments (Figure 5a). Those displaying FS phenotype (weak or non-existent sag response to square current hyperpolarization, ≥ 150 Hz firing frequency in response to square current depolarization, Figure 5b) were examined in hCSF. Recorded cells (n = 6, P18–30 rats) had an average input resistance of 126.8 ± 11.8 MΩ, sag ratio of 0.93 ± 0.02 and a maximum evoked firing frequency of 200 ± 25 Hz, measured with protocol shown in 5b. These results are similar to properties reported for FS CA1 interneurons during intact synaptic transmission (Bjorefeldt et al., 2016).

We searched for intrinsic gamma resonance using two different stimulus protocols delivered at near-threshold membrane potential as done previously (Pike et al., 2000). In the first protocol, sinusoidal current waveforms were injected at frequencies of 5, 40 and 100 Hz, for 5 s, in increments of 10 pA starting from -60 mV (Figure 5c). If the FS CA1 interneurons were selectively resonant at gamma frequency range, we expected their subthreshold voltage response to 40 Hz sinusoidal current stimulus to generate the highest impedance magnitude profile in these experiments. As seen in

Figure 4d, the impedance amplitude profile of examined cells showed no evidence of gamma frequency input preference, and this was not altered by hCSF. Impedance magnitudes in aCSF and hCSF were 94.8 ± 6.6 vs 81.6 ± 4.9 MΩ at 5 Hz (n = 6, P = 0.072, Student's paired t-test), 33.3 ± 1.6 vs 34.5 ± 2 MΩ at 40 Hz (n = 6, P = 0.48, Student's paired t-test) and 19.9 ± 1.3 vs 21.2 ± 1.6 MΩ at 100 Hz (n = 6, P = 0.13, Student's paired t-test).

However, since the gamma frequency range spans approximately 30–80 Hz, it is possible that none of the examined interneurons had resonance frequencies precisely around 40 Hz. We thus used a second protocol where a ZAP current waveform encompassing 0–100 Hz (20 s, 20 pA) was injected at near-threshold potential. Cells were current-clamped 1–2 mV negative of the membrane potential at which the protocol evoked one or more action potentials. As shown in Figure 5e-f, this protocol confirmed the lack of intrinsic gamma frequency resonance in these cells in aCSF, and hCSF did not alter this. In fact, in none of the examined FS cells did the impedance magnitude in the 30-80 Hz range exceed 50% of the magnitude recorded at 0.5 Hz.

To exclude the possibility that the FS cells would, despite absence of subthreshold gamma resonance, still display firing preference to gamma frequency input, we delivered the same ZAP current protocol at suprathreshold membrane potentials (Figure 5g-h). However, as expected, firing preferentially occurred in response to low frequency (0–5 Hz) input where voltage deflections were of greatest amplitude. None of the cells firing action potentials did so selectively in the 30–80 Hz range. Although hCSF did not induce a gamma frequency input-driven firing preference in FS

interneurons, we found a significant increase in the total number of spikes per ZAP stimulus (1.5 ± 0.3 vs 7.5 ± 1.7, n = 6, P = 0.02, Student's paired t-test, Figure 5h). To confirm that the increased excitability of FS interneurons was specific to hCSF treatment, we monitored the frequency–current relationship in a mixed group of CA1 stratum pyramidale interneurons (average maximum firing frequency: 95.5 ± 22.2 Hz, range: 56-180 Hz, n = 4, P17–25 rats, protocol as in Figure 5b) over time in aCSF. All interneurons examined showed a decreased intrinsic excitability over the same time period that hCSF was applied (10-15 minutes), as indicated by fewer action potentials in response to rheobase current (minimum current injection required to evoke one or more action potentials) and lowered half-maximum and maximum firing frequencies (data not shown). Accordingly, frequency–current curves were right-shifted over time in whole-cell recordings, as shown to occur previously in CA1 pyramidal cells (Bjorefeldt et al., 2015).

This indicates that hCSF causes an increase in intrinsic excitability of FS CA1 interneurons, consistent with previous findings in rat hippocampal brain slices (Bjorefeldt et al., 2016). While we were not able to confirm the existence of intrinsic gamma frequency resonance in FS CA1 interneurons, the hCSF-mediated increase in excitability of these cells could help explain the emergence of spontaneous gamma oscillations.

## DISCUSSION

Here we show that application of hCSF to hippocampal brain slices *in vitro* promotes spontaneous network gamma oscillations in CA3 stratum pyramidale. We initially observed that hCSF strongly increased the power of KA-induced gamma oscillations,

as compared to an aCSF of matched electrolyte and glucose composition. In subsequent experiments we found that hCSF alone, without any added supplements, generated spontaneous gamma oscillations that were readily reversed by washout. hCSF-induced gamma oscillations were entirely abolished by atropine application, suggesting involvement of muscarinic acetylcholine receptor (mAChR)-mediated signaling. In search of a potential cellular mechanism of these effects we tested hippocampal pyramidal cells and FS interneurons for intrinsic gamma frequency resonance but were unable to confirm such properties at baseline (in aCSF), and hCSF did not alter this. However, we found evidence that hCSF positively modulates $I_h$ in pyramidal cells and increases the excitability of FS interneurons, revealing two plausible mechanisms that could contribute to the generation of hCSF-induced gamma oscillations. First, modulation of $I_h$ by muscarine has been shown to be a contributing factor to the generation of hippocampal gamma oscillations through activation of mACh receptors (Fisahn et al., 2002). Second, optogenetic activation of FS interneurons *in vivo* has been shown to promote the generation of cortical gamma oscillations (Cardin et al., 2009; Sohal et al., 2009).

We initially observed that hCSF increased the strength of KA-induced gamma oscillations in CA3 stratum pyramidale. Such increase in gamma power can have several mechanistic explanations. For example, an increased number of participating neurons, increased synchronization of action potential firing or a change in the balance between excitatory and inhibitory synaptic activity could all produce an increased power of the gamma oscillation (Bartos et al., 2007; Fisahn et al., 1998; Leao et al., 2009). The previously described excitability-increasing effect of hCSF on hippocampal pyramidal cells (Bjorefeldt et al., 2015) and FS interneurons (Bjorefeldt

et al., 2016) is likely to entrain more neurons into the gamma oscillation and thus increase power. KA-induced gamma oscillations are highly dependent on inhibitory transmission via $GABA_A$ receptors, but do not require intact AMPA receptor-mediated transmission as sufficient excitation is achieved through the activation of KA receptors (Fisahn et al., 2004). Because hCSF appears to excite pyramidal cells more strongly than interneurons (Bjorefeldt et al., 2016), a net increase in excitatory transmission is expected when introducing hCSF to KA-induced gamma oscillations, which may beneficially influence rhythmogenesis in the network.

The strength of the hCSF-induced gamma oscillations reported in this study was on average low compared to that normally observed after typical (100 nM) KA application to aCSF (Andersson et al., 2010; Fisahn et al., 2004; Kurudenkandy et al., 2014). While KA application at this concentration likely produces stronger excitation of hippocampal neurons compared to hCSF, other factors may contribute to the difference in gamma oscillation strength. Notably, the physiological concentration of glucose, as measured in hCSF (~3–4 mM, see Table 1), is substantially lower than what is typically used in aCSF in hippocampal brain slice studies (≥ 10 mM). Gamma oscillations are known to be associated with high metabolic demand (Galow et al., 2014; Kann, 2011) and their strength and probability of occurrence *in vitro* is known to be glucose-dependent (Galow et al., 2014). However, we chose to study the effect of hCSF on network gamma oscillations without any manipulation of its composition. It is therefore conceivable that the physiological (lower) glucose levels in hCSF partly accounted for the difference in power of hCSF-induced (spontaneous), as compared to typical KA-evoked, gamma oscillations.

Our finding that hCSF-induced gamma oscillations are entirely abolished by atropine application implies significant contribution of mAChR activation in these oscillations. Indeed, the mAChR agonists carbachol and muscarine readily evoke gamma oscillations when applied to hippocampal brain slices (Fisahn et al., 1998; Palhalmi et al., 2004). Furthermore, positive modulation of $I_h$, as observed here in CA1 pyramidal cells in hCSF, has been shown to result from mAChR activation (Colino and Halliwell, 1993; Fisahn et al., 2002). While mAChRs appear to be necessary for the maintenance of hCSF-induced gamma oscillations, it is not yet clear whether they are sufficient for their induction. We also note that we cannot exclude that constitutively active mAChRs contribute and that atropine may act as an inverse agonist. Previous observations support a role of non-cholinergic neuromodulators in hCSF effects on CA1 pyramidal cells and interneurons. For example, hCSF has been shown to strongly increase evoked excitatory synaptic transmission at CA3-CA1 synapses through an apparent increase in presynaptic release probability (Bjorefeldt et al., 2015), whereas mAChR agonists are known to supress glutamate release at these synapses (Fernandez de Sevilla and Buno, 2003).

In whole-cell recordings from CA1 pyramidal cells the enhanced theta resonance strength and somewhat increased resonance frequency observed in hCSF likely resulted from enhancement of $I_h$. This conclusion is consistent with findings in other studies where resonance frequency and strength increase with stronger activation of this conductance (Hu et al., 2002; Narayanan and Johnston, 2008). We found no evidence of gamma resonance in CA1 pyramidal cells in either aCSF or hCSF, which is in agreement with previous studies (Pike et al., 2000; Zemankovics et al.,

2010). However, our results in CA1 pyramidal cells suggest hCSF may also promote the induction of spontaneous theta network oscillations in the hippocampus, which should be addressed in future studies. However, in horizontally sectioned hippocampal slices the preserved microcircuitry is believed to favour the induction of gamma, rather than theta, oscillations (Boehlen et al., 2009; Gloveli et al., 2005). While CSF neuromodulators could ultimately serve to promote both gamma and theta network oscillations in the hippocampus *in vivo*, the differentially preserved connectivity in the *in vitro* slice preparation could explain why gamma and not theta network activity was observed in hCSF in this study.

In addition to effects on theta resonance, potentiation of $I_h$ could also serve to increase the coherence of action potential firing among CA1, and presumably CA3, pyramidal cells. As the pyramidal cells recover from synaptic inhibition during the gamma oscillation cycle, an increased $I_h$ conductance may promote synchronization of rebound firing (Gastrein et al., 2011). Further supporting a role of $I_h$ in gamma rhythmogenesis is the finding that application of ZD7288 (a selective $I_h$-blocker) causes a profound decrease in the power of hippocampal gamma oscillations *in vitro* (Boehlen et al., 2009; Leao et al., 2009). $I_h$ is also present, to varying degree, in hippocampal interneurons (Aponte et al., 2006; Cooper et al., 2001; Rotstein et al., 2005), where similar modulation by hCSF could further promote synchronization of action potential firing.

In the present study, we could not find evidence of intrinsic gamma frequency resonance in FS CA1 interneurons, as was previously described *in vitro* (Pike et al., 2000). In fact, at near threshold membrane potential all examined FS interneurons

were non-resonant over the entire 0–100 Hz frequency span. Notable discrepancies between our study and that of Pike et al. (2000) are the higher recording temperature (32–34 °C), physiological (lower) glucose concentration and presence of synaptic blockers (AP-5, CNQX and picrotoxin) in the present study. Although FS interneurons are associated with high metabolic demand (Kann et al., 2014), the lower extracellular glucose concentration used in our recordings is unlikely to explain lack of gamma resonance since cells were also supplemented with ATP through the recording pipette. Neither should the use of synaptic blockers mask an intrinsic resonance previously shown to depend on voltage-gated sodium channels (Pike et al., 2000). It is possible, however, that a subset of FS interneurons could display intrinsic gamma resonance, and that we did not sample that subpopulation in our experiments.

While often assumed to contribute in the generation and/or maintenance of network gamma oscillations, the significance and precise function of intrinsic gamma resonance, if present in FS interneurons *in vivo*, is not well established. In fact, other cellular mechanisms may better explain how these cells assist gamma rhythmogenesis in neural networks. Because FS interneurons are known to form strong inhibitory autapses (Bacci et al., 2003; Deleuze et al., 2014; Tamas et al., 1997), each firing event is expected to impose swift self-inhibition lasting for a time period corresponding to the decay time of the $GABA_A$-ergic inhibitory postsynaptic potential (20–30 milliseconds). Assuming a sufficient persistent level of excitatory synaptic input, this provides a mechanism to explain how FS interneurons could fire at gamma frequency *in vivo* and *in vitro* in absence of gamma resonance. If not essential in gamma rhythmogenesis, an alternative function of gamma resonance in

FS interneurons might be to stabilize ongoing gamma oscillations from perturbation by unsynchronized activity (noise), as was recently suggested (Tikidji-Hamburyan et al., 2015). Thus, assuming complete absence of intrinsic gamma resonance across the entire hippocampal FS cell population, hCSF could induce spontaneous gamma oscillations by sufficiently increasing the excitability of hippocampal pyramidal cells and interneurons (LeBeau et al., 2002), as is indicated in the present study and extensively described in Bjorefeldt et al. (2015, 2016).

We conclude that application of hCSF to hippocampal brain slices induces network gamma oscillations *in vitro*. This finding opens up the possibility of studying these oscillations under more *in vivo*–like conditions in both health and disease. In future work, the specific cellular and molecular requirements of hCSF-induced gamma oscillations should be examined in greater detail, as well as the effect of hCSF on other hippocampal network activity patterns such as theta and sharp-wave ripple oscillations.

## REFERENCES


Andersson R, Lindskog M, Fisahn A. 2010. Histamine H3 receptor activation decreases kainate-induced hippocampal gamma oscillations in vitro by action potential desynchronization in pyramidal neurons. J Physiol 588(Pt 8):1241-9.

Aponte Y, Lien CC, Reisinger E, Jonas P. 2006. Hyperpolarization-activated cation channels in fast-spiking interneurons of rat hippocampus. J Physiol 574(Pt 1):229-43.

Bacci A, Huguenard JR, Prince DA. 2003. Functional autaptic neurotransmission in fast-spiking interneurons: a novel form of feedback inhibition in the neocortex. J Neurosci 23(3):859-66.

Bartos M, Vida I, Jonas P. 2007. Synaptic mechanisms of synchronized gamma oscillations in inhibitory interneuron networks. Nat Rev Neurosci 8(1):45-56.

Beshel J, Kopell N, Kay LM. 2007. Olfactory bulb gamma oscillations are enhanced with task demands. J Neurosci 27(31):8358-65.

Bjorefeldt A, Andreasson U, Daborg J, Riebe I, Wasling P, Zetterberg H, Hanse E. 2015. Human cerebrospinal fluid increases the excitability of pyramidal neurons in the in

679 vitro brain slice. J Physiol.
680 Bjorefeldt A, Wasling P, Zetterberg H, Hanse E. 2016. Neuromodulation of fast-spiking and
681 non-fast-spiking hippocampal CA1 interneurons by human cerebrospinal fluid. J
682 Physiol 594(4):937-52.
683 Boddeke HW, Best R, Boeijinga PH. 1997. Synchronous 20 Hz rhythmic activity in
684 hippocampal networks induced by activation of metabotropic glutamate receptors in
685 vitro. Neuroscience 76(3):653-8.
686 Boehlen A, Kunert A, Heinemann U. 2009. Effects of XE991, retigabine, losigamone and
687 ZD7288 on kainate-induced theta-like and gamma network oscillations in the rat
688 hippocampus in vitro. Brain Res 1295:44-58.
689 Buzsaki G. 2006. Rhythms of the brain: Oxford Univesity Press.
690 Buzsaki G, Draguhn A. 2004. Neuronal oscillations in cortical networks. Science
691 304(5679):1926-9.
692 Buzsaki G, Wang XJ. 2012. Mechanisms of gamma oscillations. Annu Rev Neurosci 35:203-
693 25.
694 Cardin JA. 2016. Snapshots of the Brain in Action: Local Circuit Operations through the
695 Lens of gamma Oscillations. J Neurosci 36(41):10496-10504.
696 Cardin JA, Carlen M, Meletis K, Knoblich U, Zhang F, Deisseroth K, Tsai LH, Moore CI.
697 2009. Driving fast-spiking cells induces gamma rhythm and controls sensory
698 responses. Nature 459(7247):663-7.
699 Colino A, Halliwell JV. 1993. Carbachol potentiates Q current and activates a calcium-
700 dependent non-specific conductance in rat hippocampus in vitro. Eur J Neurosci
701 5(9):1198-209.
702 Cooper EC, Harrington E, Jan YN, Jan LY. 2001. M channel KCNQ2 subunits are localized
703 to key sites for control of neuronal network oscillations and synchronization in mouse
704 brain. J Neurosci 21(24):9529-40.
705 Deleuze C, Pazienti A, Bacci A. 2014. Autaptic self-inhibition of cortical GABAergic
706 neurons: synaptic narcissism or useful introspection? Curr Opin Neurobiol 26:64-71.
707 Dickinson R, Awaiz S, Whittington MA, Lieb WR, Franks NP. 2003. The effects of general
708 anaesthetics on carbachol-evoked gamma oscillations in the rat hippocampus in vitro.
709 Neuropharmacology 44(7):864-72.
710 Fernandez de Sevilla D, Buno W. 2003. Presynaptic inhibition of Schaffer collateral synapses
711 by stimulation of hippocampal cholinergic afferent fibres. Eur J Neurosci 17(3):555-
712 8.
713 Fisahn A. 2005. Kainate receptors and rhythmic activity in neuronal networks: hippocampal
714 gamma oscillations as a tool. J Physiol 562(Pt 1):65-72.
715 Fisahn A, Contractor A, Traub RD, Buhl EH, Heinemann SF, McBain CJ. 2004. Distinct
716 roles for the kainate receptor subunits GluR5 and GluR6 in kainate-induced
717 hippocampal gamma oscillations. J Neurosci 24(43):9658-68.
718 Fisahn A, Pike FG, Buhl EH, Paulsen O. 1998. Cholinergic induction of network oscillations
719 at 40 Hz in the hippocampus in vitro. Nature 394(6689):186-9.
720 Fisahn A, Yamada M, Duttaroy A, Gan JW, Deng CX, McBain CJ, Wess J. 2002. Muscarinic
721 induction of hippocampal gamma oscillations requires coupling of the M1 receptor to
722 two mixed cation currents. Neuron 33(4):615-24.
723 Flint AC, Connors BW. 1996. Two types of network oscillations in neocortex mediated by
724 distinct glutamate receptor subtypes and neuronal populations. J Neurophysiol
725 75(2):951-7.
726 Fries P. 2015. Rhythms for Cognition: Communication through Coherence. Neuron
727 88(1):220-35.
728 Fuchs EC, Zivkovic AR, Cunningham MO, Middleton S, Lebeau FE, Bannerman DM,

729 Rozov A, Whittington MA, Traub RD, Rawlins JN and others. 2007. Recruitment of
730 parvalbumin-positive interneurons determines hippocampal function and associated
731 behavior. Neuron 53(4):591-604.
732 Galow LV, Schneider J, Lewen A, Ta TT, Papageorgiou IE, Kann O. 2014. Energy substrates
733 that fuel fast neuronal network oscillations. Front Neurosci 8:398.
734 Gastrein P, Campanac E, Gasselin C, Cudmore RH, Bialowas A, Carlier E, Fronzaroli-
735 Molinieres L, Ankri N, Debanne D. 2011. The role of hyperpolarization-activated
736 cationic current in spike-time precision and intrinsic resonance in cortical neurons in
737 vitro. J Physiol 589(Pt 15):3753-73.
738 Gloveli T, Dugladze T, Rotstein HG, Traub RD, Monyer H, Heinemann U, Whittington MA,
739 Kopell NJ. 2005. Orthogonal arrangement of rhythm-generating microcircuits in the
740 hippocampus. Proc Natl Acad Sci U S A 102(37):13295-300.
741 Hu H, Vervaeke K, Storm JF. 2002. Two forms of electrical resonance at theta frequencies,
742 generated by M-current, h-current and persistent Na+ current in rat hippocampal
743 pyramidal cells. J Physiol 545(Pt 3):783-805.
744 Joborn C, Hetta J, Niklasson F, Rastad J, Wide L, Agren H, Akerstrom G, Ljunghall S. 1991.
745 Cerebrospinal fluid calcium, parathyroid hormone, and monoamine and purine
746 metabolites and the blood-brain barrier function in primary hyperparathyroidism.
747 Psychoneuroendocrinology 16(4):311-22.
748 Kann O. 2011. The energy demand of fast neuronal network oscillations: insights from brain
749 slice preparations. Front Pharmacol 2:90.
750 Kann O, Papageorgiou IE, Draguhn A. 2014. Highly energized inhibitory interneurons are a
751 central element for information processing in cortical networks. J Cereb Blood Flow
752 Metab 34(8):1270-82.
753 Kurudenkandy FR, Zilberter M, Biverstal H, Presto J, Honcharenko D, Stromberg R,
754 Johansson J, Winblad B, Fisahn A. 2014. Amyloid-beta-induced action potential
755 desynchronization and degradation of hippocampal gamma oscillations is prevented
756 by interference with peptide conformation change and aggregation. J Neurosci
757 34(34):11416-25.
758 Leao RN, Tan HM, Fisahn A. 2009. Kv7/KCNQ channels control action potential phasing of
759 pyramidal neurons during hippocampal gamma oscillations in vitro. J Neurosci
760 29(42):13353-64.
761 LeBeau FE, Towers SK, Traub RD, Whittington MA, Buhl EH. 2002. Fast network
762 oscillations induced by potassium transients in the rat hippocampus in vitro. J Physiol
763 542(Pt 1):167-79.
764 Lisman JE, Jensen O. 2013. The theta-gamma neural code. Neuron 77(6):1002-16.
765 Maccaferri G, McBain CJ. 1996. The hyperpolarization-activated current (Ih) and its
766 contribution to pacemaker activity in rat CA1 hippocampal stratum oriens-alveus
767 interneurones. J Physiol 497 ( Pt 1):119-30.
768 Mann EO, Suckling JM, Hajos N, Greenfield SA, Paulsen O. 2005. Perisomatic feedback
769 inhibition underlies cholinergically induced fast network oscillations in the rat
770 hippocampus in vitro. Neuron 45(1):105-17.
771 Narayanan R, Johnston D. 2008. The h channel mediates location dependence and plasticity
772 of intrinsic phase response in rat hippocampal neurons. J Neurosci 28(22):5846-60.
773 Palhalmi J, Paulsen O, Freund TF, Hajos N. 2004. Distinct properties of carbachol- and
774 DHPG-induced network oscillations in hippocampal slices. Neuropharmacology
775 47(3):381-9.
776 Pape HC. 1996. Queer current and pacemaker: the hyperpolarization-activated cation current
777 in neurons. Annu Rev Physiol 58:299-327.
778 Pike FG, Goddard RS, Suckling JM, Ganter P, Kasthuri N, Paulsen O. 2000. Distinct

779 frequency preferences of different types of rat hippocampal neurones in response to
780 oscillatory input currents. J Physiol 529 Pt 1:205-13.
781 Puil E, Gimbarzevsky B, Miura RM. 1986. Quantification of membrane properties of
782 trigeminal root ganglion neurons in guinea pigs. J Neurophysiol 55(5):995-1016.
783 Rotstein HG, Pervouchine DD, Acker CD, Gillies MJ, White JA, Buhl EH, Whittington MA,
784 Kopell N. 2005. Slow and fast inhibition and an H-current interact to create a theta
785 rhythm in a model of CA1 interneuron network. J Neurophysiol 94(2):1509-18.
786 Sederberg PB, Schulze-Bonhage A, Madsen JR, Bromfield EB, McCarthy DC, Brandt A,
787 Tully MS, Kahana MJ. 2007. Hippocampal and neocortical gamma oscillations
788 predict memory formation in humans. Cereb Cortex 17(5):1190-6.
789 Singer W. 1999. Neuronal synchrony: a versatile code for the definition of relations? Neuron
790 24(1):49-65, 111-25.
791 Sohal VS. 2016. How Close Are We to Understanding What (if Anything) gamma
792 Oscillations Do in Cortical Circuits? J Neurosci 36(41):10489-10495.
793 Sohal VS, Zhang F, Yizhar O, Deisseroth K. 2009. Parvalbumin neurons and gamma rhythms
794 enhance cortical circuit performance. Nature 459(7247):698-702.
795 Tamas G, Buhl EH, Somogyi P. 1997. Massive autaptic self-innervation of GABAergic
796 neurons in cat visual cortex. J Neurosci 17(16):6352-64.
797 Taylor K, Mandon S, Freiwald WA, Kreiter AK. 2005. Coherent oscillatory activity in
798 monkey area v4 predicts successful allocation of attention. Cereb Cortex 15(9):1424-
799 37.
800 Tikidji-Hamburyan RA, Martinez JJ, White JA, Canavier CC. 2015. Resonant Interneurons
801 Can Increase Robustness of Gamma Oscillations. J Neurosci 35(47):15682-95.
802 Traub RD, Whittington MA, Colling SB, Buzsaki G, Jefferys JG. 1996. Analysis of gamma
803 rhythms in the rat hippocampus in vitro and in vivo. J Physiol 493 ( Pt 2):471-84.
804 Vandecasteele M, Varga V, Berenyi A, Papp E, Bartho P, Venance L, Freund TF, Buzsaki G.
805 2014. Optogenetic activation of septal cholinergic neurons suppresses sharp wave
806 ripples and enhances theta oscillations in the hippocampus. Proc Natl Acad Sci U S A
807 111(37):13535-40.
808 Whittington MA, Traub RD, Jefferys JG. 1995. Synchronized oscillations in interneuron
809 networks driven by metabotropic glutamate receptor activation. Nature
810 373(6515):612-5.
811 Yamamoto J, Suh J, Takeuchi D, Tonegawa S. 2014. Successful execution of working
812 memory linked to synchronized high-frequency gamma oscillations. Cell 157(4):845-
813 57.
814 Zemankovics R, Kali S, Paulsen O, Freund TF, Hajos N. 2010. Differences in subthreshold
815 resonance of hippocampal pyramidal cells and interneurons: the role of h-current and
816 passive membrane characteristics. J Physiol 588(Pt 12):2109-32.
817

## TABLES

**Table 1.** Measured variables in hCSF and aCSF. Electrolyte and glucose concentrations in mmol/L.

| | **pH** | **Osmolality** (mOsm/Kg) | **$Na^+$** | **$K^+$** | **$Cl^-$** | **$Ca^{2+}$** | **$Mg^{2+}$** | **Glucose** |
|---|---|---|---|---|---|---|---|---|
| **hCSF** | 7.34 ± <0.01 | 293 ± 1 | 148.7 ± 1 | 2.86 ± 0.04 | 125.8 ± 1.7 | 1.13 ± 0.03 | 1.09 ± 0.03 | 3.95 ± 0.12 |
| **hCSF[1]** | 7.35 | 290 | 145.9 | 2.8 | 121.5 | 1.07 | 1.04 | 3.8 |
| **aCSF[1]** | 7.4 ± 0.01 | 286 ± 0.3 | 146.7 ± 0.3 | 2.88 ± <0.01 | 124.7 ± 0.2 | 1.10 ± <0.01 | 1.02 ± <0.01 | 3.87 ± 0.01 |

**hCSF**: Values (mean ± sem) from all hCSF pools used in the study (n = 4 pools).

**hCSF[1]**: Values obtained from one of the hCSF pools constructed from NPH patient samples.

**aCSF[1]**: Values (mean ± sem) from aCSF solutions (n = 10), prepared on separate experimental days, designed to match the electrolyte and glucose composition of hCSF[2],

## FIGURE LEGENDS

**Figure 1. hCSF strengthens kainate-evoked gamma oscillations in the hippocampal network.** (**a**) Example traces of gamma oscillations evoked by application of 45 nM kainate (KA) in aCSF (red), and after introducing hCSF supplemented with the same concentration of KA (blue). (**b**) Power spectrum computed from recordings shown in **a**. (**c**) Summary bar graph of average gamma oscillation power recorded in aCSF during step application of KA at 25 nM (dark grey), 35 nM (bright grey), 45 nM (red) and in hCSF + 45 nM KA (blue). *** $P < 0.001$. Data presented as mean ± sem.

**Figure 2. hCSF promotes spontaneous gamma oscillations in the hippocampal network.** (**a**) Example traces of spontaneous activity recorded in aCSF (black), 20 min after wash-in of hCSF (blue) and following 30 min of washout (grey) in hippocampal area CA3. (**b**) Power spectra obtained from recordings shown in **a**. (**c**) Summary bar graph showing average gamma oscillation power recorded in aCSF, in hCSF and following washout. (**d**) Example traces of spontaneous activity recorded in aCSF (black), 20 min after wash-in of hCSF (blue) and following 30 min of washout (grey) in hippocampal area CA1. (**e**) Power spectra obtained from recordings shown in **d**. (**f**) Summary bar graph showing average gamma oscillation power recorded in aCSF, in hCSF and following washout.

**Figure 3. Spontaneous gamma oscillations induced by hCSF are abolished by atropine.** (**a**) Example traces of spontaneous LFP activity recorded after exposing hippocampal slices to hCSF for 30 min (blue), and following 5 min of atropine

application (green). (**b**) Power spectrum obtained from recordings in **a**. (**c**) Summary bar graph showing average gamma power in hCSF, and after atropine application. *** P < 0.001. Data presented as mean ± sem.

**Figure 4. hCSF enhances theta resonance and increases $I_h$-amplitude in hippocampal pyramidal cells.** (**a**) Example traces showing the voltage response of a CA1 pyramidal cell to ZAP current injection at theta frequency range (0-15 Hz) in aCSF (red) and hCSF (blue). (**b**) Impedance magnitude profile constructed from traces in **a**. Dotted vertical lines indicate the resonance frequency of the cell in aCSF (red) and hCSF (blue). (**c**) Summary bar graph of the effect of hCSF on resonance frequency. (**d**) Summary graph showing the effect of hCSF on resonance strength (Q-value). (**e**) Example traces showing the voltage response of a CA1 pyramidal cell to ZAP current injection at gamma frequency range (20-60 Hz) in aCSF (red) and hCSF (blue). (**f**) Impedance magnitude profile constructed from traces shown in **e**. Note the absence of resonance. (**g**) Example traces showing h-current activation elicited by hyperpolarizing voltage commands in aCSF (red) and hCSF (blue), using voltage-clamp protocol in black. (**h**) Activation curve constructed from the voltage-clamp protocol in **g**, showing no effect of hCSF (blue) on the voltage-dependence of h-current activation in the range of -80 to -120 mV. (**i**) Summary bar graph showing normalized effect of hCSF on h-current amplitude. * P < 0.05. Data presented as mean ± sem.

**Figure 5. hCSF does not alter lack of intrinsic gamma frequency resonance but increases the excitability of hippocampal fast-spiking interneurons.** (**a**) Schematic drawing indicating the position of cell somata (black), with respect to the

pyramidal cell layer (grey), in whole-cell recordings from fast-spiking CA1 interneurons. Str. ori: stratum oriens, str. pyr: stratum pyramidale, str. rad: stratum radiatum (**b**) Typical electrophysiological response of an interneuron classified as fast-spiking to hyperpolarizing and depolarizing step current injection. (**c**) Oscillatory input current protocols (in black, 20 pA, 5 seconds, truncated for clarity) and subsequent voltage responses in aCSF (red) and hCSF (blue). (**d**) Summary graph showing the average impedance magnitude recorded at 5, 40, and 100 Hz in aCSF (red) and hCSF (blue). (**e**) Example traces showing the voltage response of a CA1 fast-spiking interneuron to ZAP current injection (0-100 Hz, 20 pA, 20 seconds) at near-threshold membrane potential in aCSF (red) and hCSF (blue). (**f**) Impedance magnitude profiles constructed from the ZAP current protocol in **e**. Average impedance magnitude of fast-spiking interneurons (n = 6) in aCSF (dark red) and hCSF (dark blue). Insets show average impedance magnitude at 20-60 Hz in in aCSF (dark red) and hCSF (dark blue). Note absence of gamma resonance in both aCSF and hCSF. (**g**) Example traces showing suprathreshold response of fast-spiking interneurons to same ZAP current stimulus as in **e**, in aCSF (red) and hCSF (blue). Note absence of firing preference in gamma range (30-80 Hz, grey bar at bottom) (**h**) Scatter dot plot showing number of spikes elicited by each cell in aCSF and hCSF from the ZAP current stimulus. * $P < 0.05$. Data presented as mean ± sem.

Figure 1

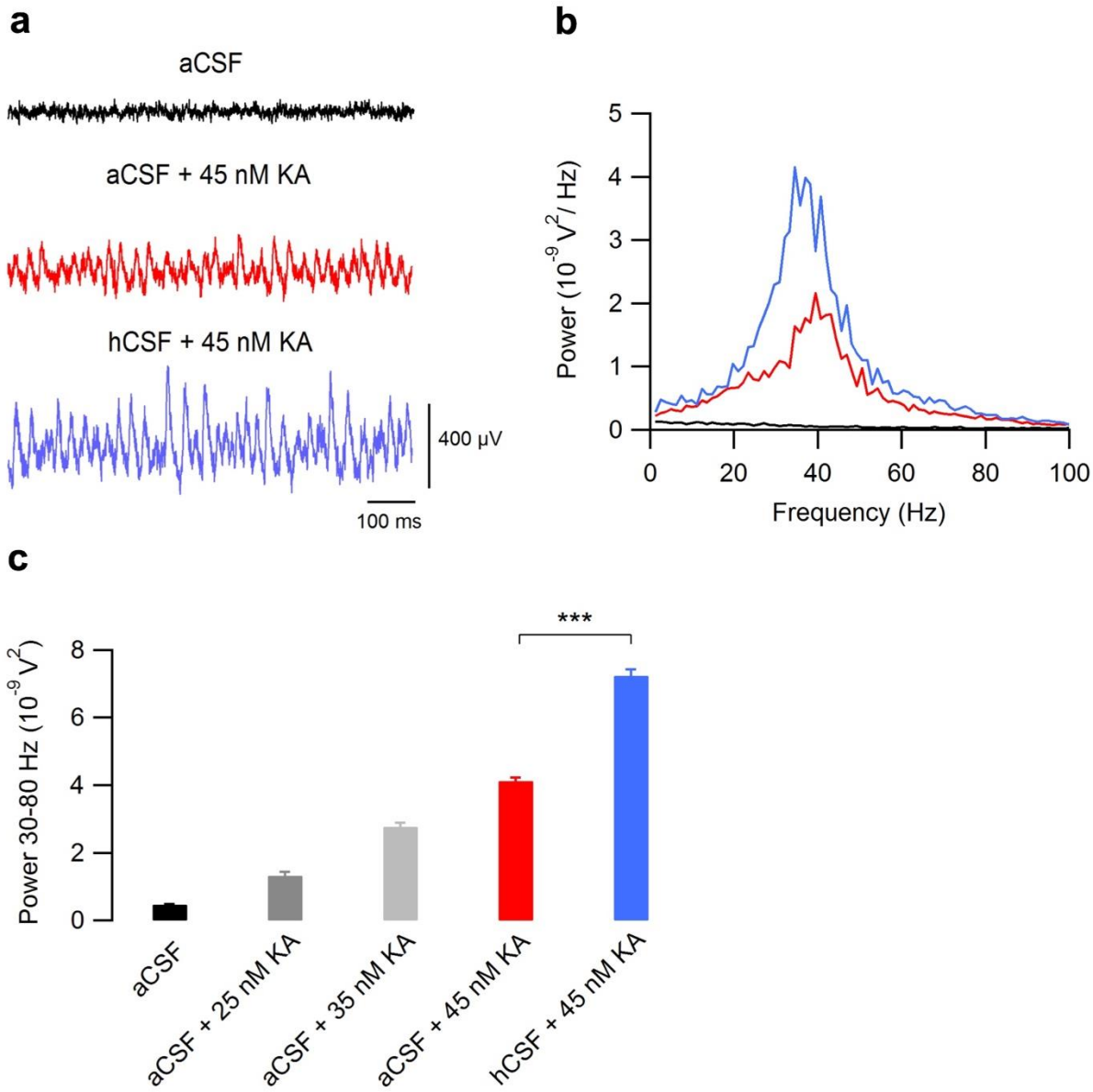
a
aCSF
aCSF + 45 nM KA
hCSF + 45 nM KA
400 µV
100 ms
b
Power (10-9 V2/ Hz)
Frequency (Hz)
c
Power 30-80 Hz (10-9 V2)
***
aCSF
aCSF + 25 nM KA
aCSF + 35 nM KA
aCSF + 45 nM KA
hCSF + 45 nM KA

Figure 2

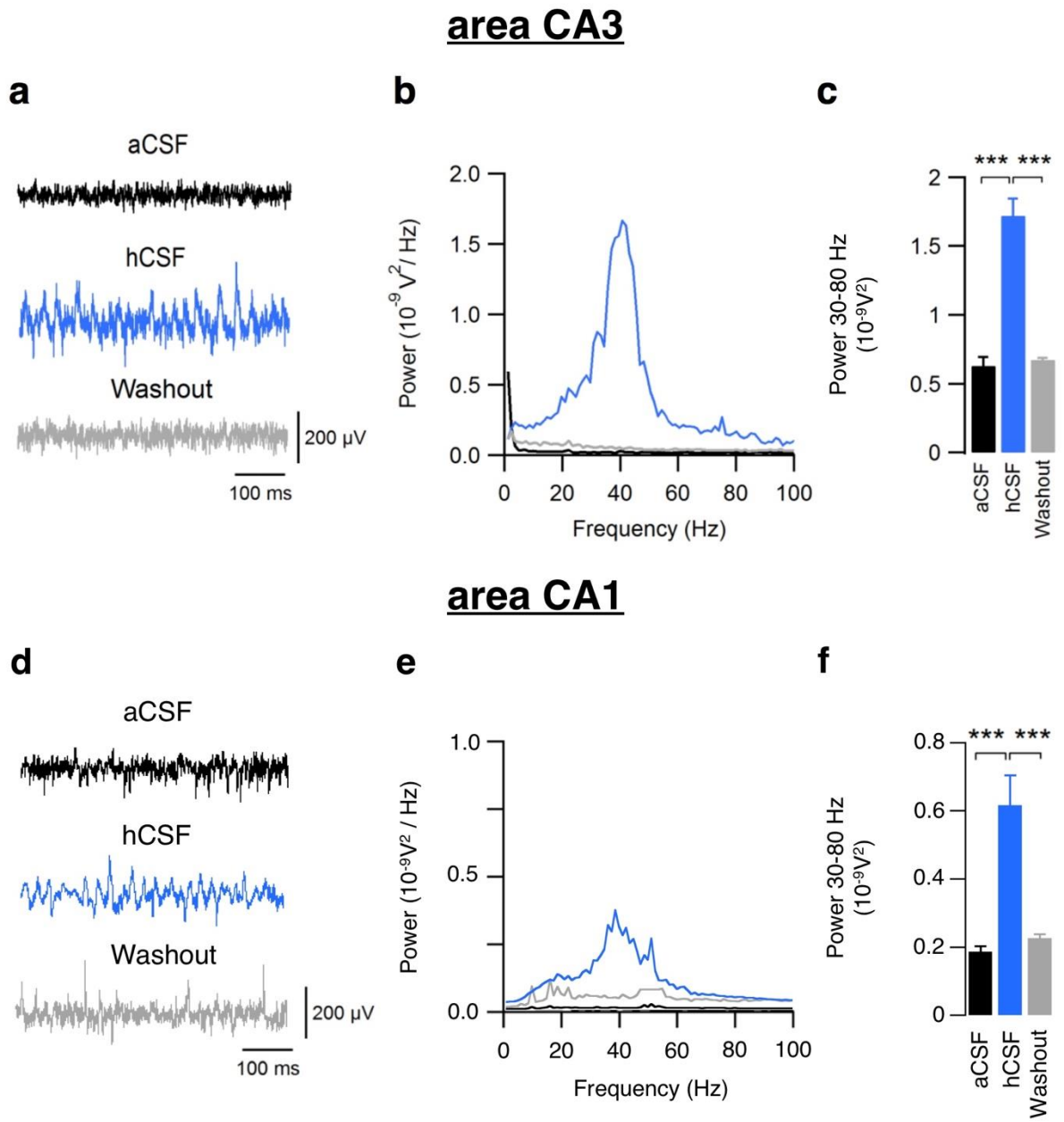
area CA3
a
aCSF
hCSF
Washout
200 µV
100 ms
b
Power (10⁻⁹ V²/ Hz)
2.0
1.5
1.0
0.5
0.0
0
20
40
60
80
100
Frequency (Hz)
c
Power 30-80 Hz (10⁻⁹V²)
***
***
2
1.5
1
0.5
0
aCSF
hCSF
Washout
area CA1
d
aCSF
hCSF
Washout
200 µV
100 ms
e
Power (10⁻⁹V² / Hz)
1.0
0.5
0.0
0
20
40
60
80
100
Frequency (Hz)
f
Power 30-80 Hz (10⁻⁹V²)
***
***
0.8
0.6
0.4
0.2
0
aCSF
hCSF
Washout

907 Figure 3

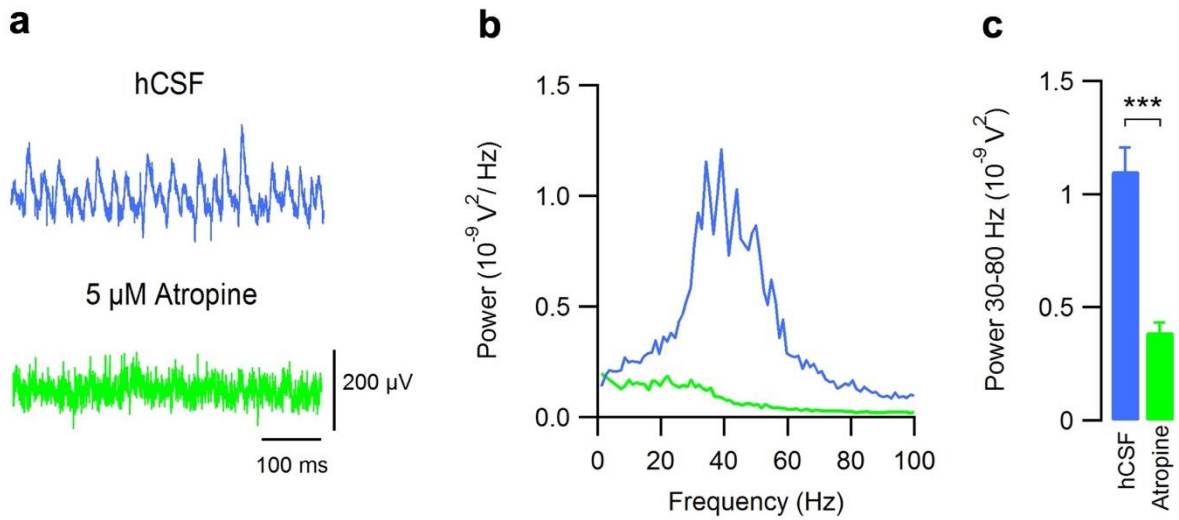


908

909

Figure 4

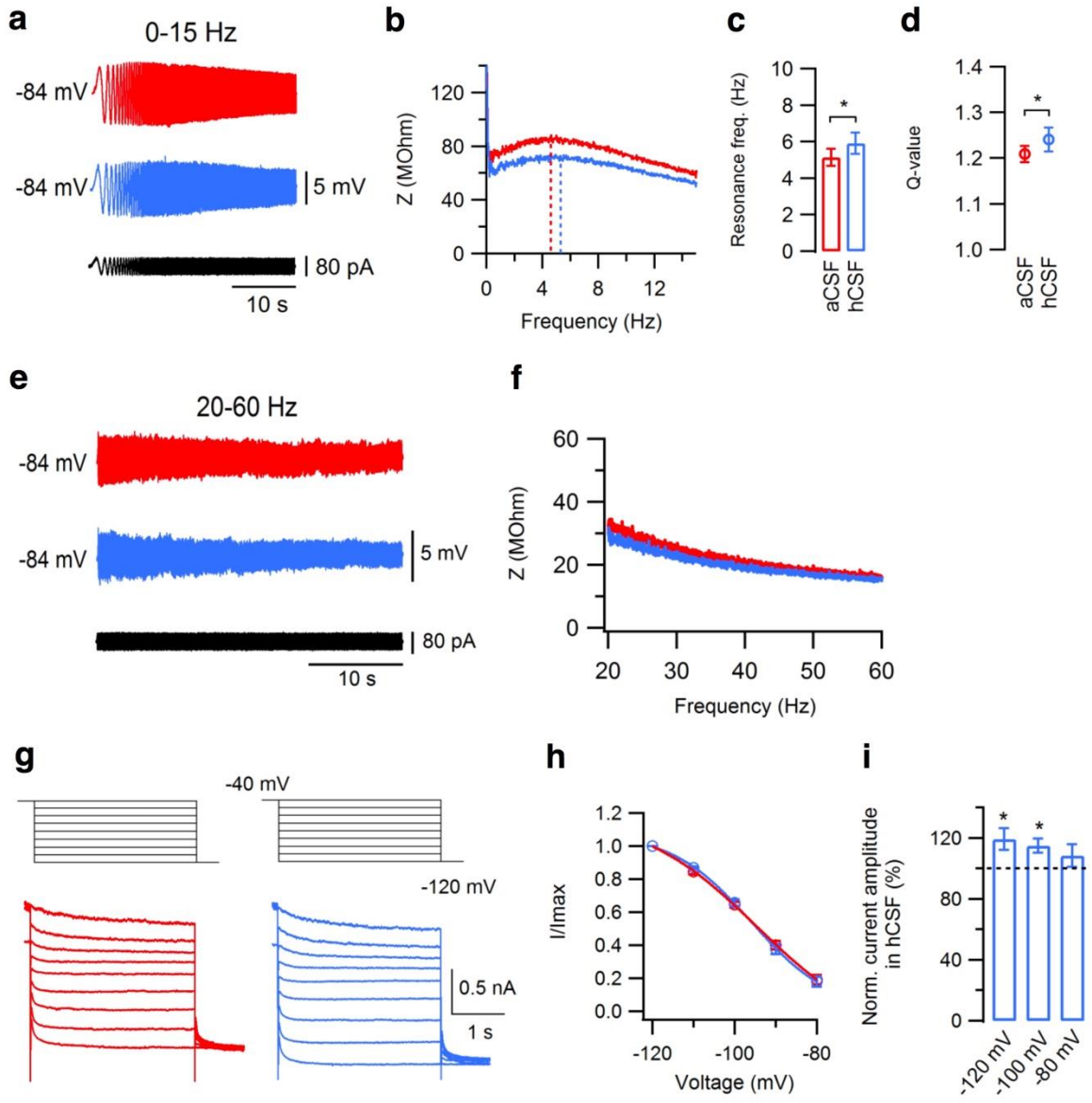
a
0-15 Hz
-84 mV
-84 mV
5 mV
80 pA
10 s
b
Z (MOhm)
Frequency (Hz)
c
Resonance freq. (Hz)
aCSF
hCSF
d
Q-value
aCSF
hCSF
e
20-60 Hz
-84 mV
-84 mV
5 mV
80 pA
10 s
f
Z (MOhm)
Frequency (Hz)
g
-40 mV
-120 mV
0.5 nA
1 s
h
I/Imax
Voltage (mV)
i
Norm. current amplitude in hCSF (%)
-120 mV
-100 mV
-80 mV

Figure 5

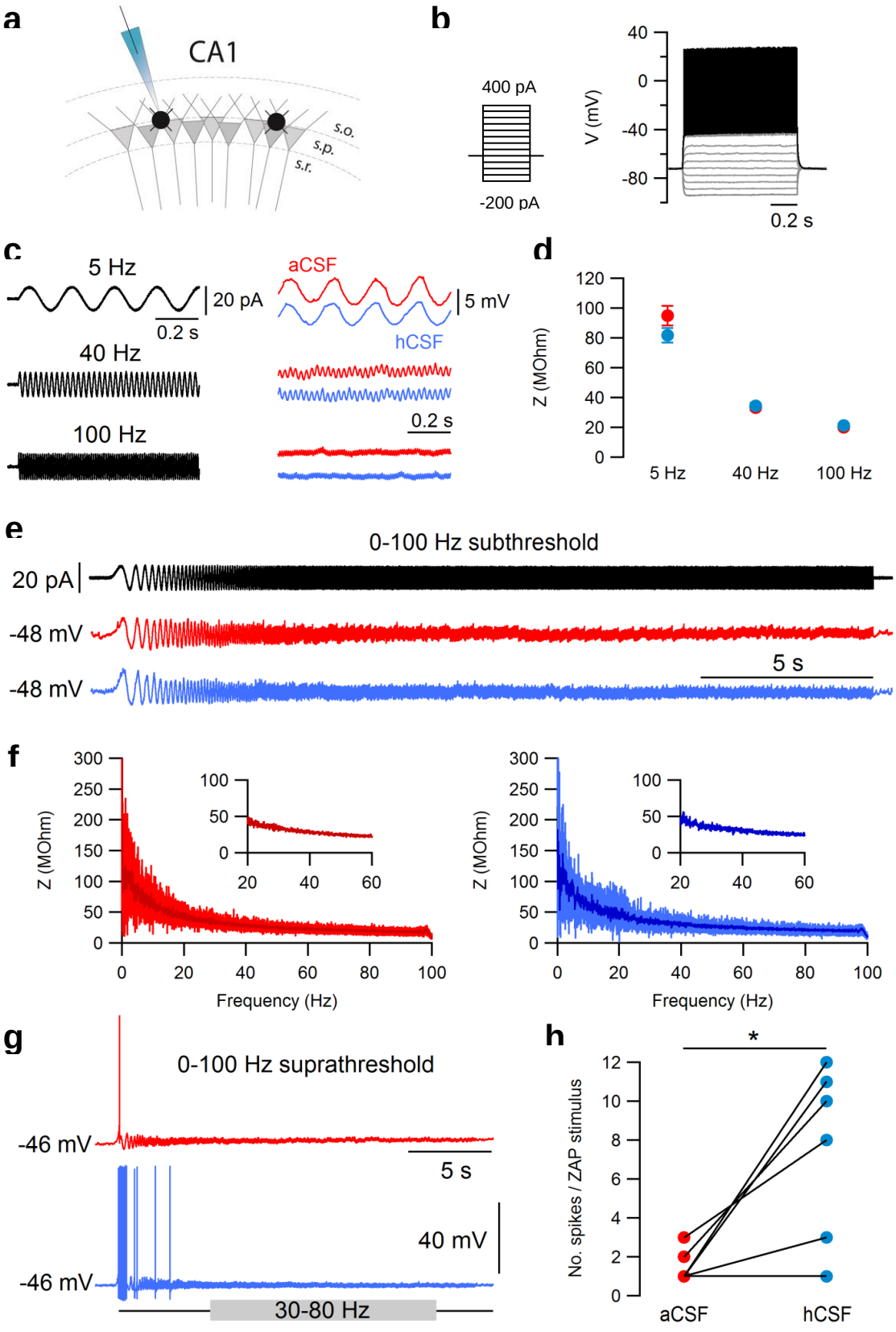
a
CA1
s.o.
s.p.
s.r.
b
400 pA
-200 pA
V (mV)
40
0
-40
-80
0.2 s
c
5 Hz
20 pA
0.2 s
40 Hz
100 Hz
aCSF
5 mV
hCSF
0.2 s
d
Z (MOhm)
120
100
80
60
40
20
0
5 Hz
40 Hz
100 Hz
e
0-100 Hz subthreshold
20 pA
-48 mV
-48 mV
5 s
f
Z (MOhm)
Frequency (Hz)
g
0-100 Hz suprathreshold
-46 mV
5 s
40 mV
-46 mV
30-80 Hz
h
*
No. spikes / ZAP stimulus
aCSF
hCSF